APRIL: Approximating Polygons as Raster Interval Lists

Thanasis Georgiadis
University of Ioannina, Greece
Greece
ageorgiadis@cs.uoi.gr

Eleni Tzirita Zacharatou
IT University of Copenhagen
Denmark
elza@itu.dk

Nikos Mamoulis
University of Ioannina, Greece
Greece
nikos@cs.uoi.gr

ABSTRACT

The spatial intersection join an important spatial query operation, due to its popularity and high complexity. The spatial join pipeline takes as input two collections of spatial objects (e.g., polygons). In the filter step, pairs of object MBRs that intersect are identified and passed to the refinement step for verification of the join predicate on the exact object geometries. The bottleneck of spatial join evaluation is in the refinement step. We introduce APRIL, a powerful intermediate step in the pipeline, which is based on raster interval approximations of object geometries. Our technique applies a sequence of interval joins on "intervalized" object approximations to determine whether the objects intersect or not. Compared to previous work, APRIL approximations are simpler, occupy much less space, and achieve similar pruning effectiveness at a much higher speed. Besides intersection joins between polygons, APRIL can directly be applied and has high effectiveness for polygonal range queries, within joins, and polygon-linestring joins. By applying a lightweight compression technique, APRIL approximations may occupy even less space than object MBRs. Furthermore, APRIL can be customized to apply on partitioned data and on polygons of varying sizes, rasterized at different granularities. Our last contribution is a novel algorithm that computes the APRIL approximation of a polygon without having to rasterize it in full, which is orders of magnitude faster than the computation of other raster approximations. Experiments on real data demonstrate the effectiveness and efficiency of APRIL; compared to the state-of-the-art intermediate filter, APRIL occupies 2x-8x less space, is 3.5x-8.5x more time-efficient, and reduces the end-to-end join cost up to 3 times.

PVLDB Reference Format:
Thanasis Georgiadis, Eleni Tzirita Zacharatou, and Nikos Mamoulis. APRIL: Approximating Polygons as Raster Interval Lists. PVLDB, 14(1): XXX-XXX, 2020.
doi:XX.XX/XXX.XX

PVLDB Artifact Availability:
The source code, data, and/or other artifacts have been made available at https://github.com/ThanGeo/APRIL.

1 INTRODUCTION

We study the problem of computing the spatial intersection join between two spatial object collections R and S, which identifies all pairs of objects $(r, s), r \in R, s \in S$ such that r shares at least one common point with s. Besides being a common operation in geographic information systems (GIS), the spatial intersection join finds a wide range of applications in geo-spatial interlinking [34], GeoSPARQL queries on RDF data stores [45], interference detection between objects in computer graphics [37], suggestion of synapses between neurons in neuroscience models [30]. Recently, there is a growing interest in spatial query evaluation over complex object geometries (i.e., polygons) [15, 16, 19, 23, 29, 32, 38, 44, 49, 53, 54].

A naive way to evaluate the join is to run an intersection test algorithm from computational geometry for each pair (r, s) in $R \times S$. However, this method is extremely expensive, since (i) the number $|R \times S|$ of pairs to be tested can be huge and (ii) for each pair the test takes $O(n \log n)$ time [10]. To mitigate (i), the join is evaluated in two steps. Provided that the minimum bounding rectangles (MBRs) of the objects are available (and possibly indexed), in the *filter step*, an efficient MBR-join algorithm [11, 47] is used to find the pairs of objects $(r, s) \in R \times S$ such that $MBR(r)$ intersects with $MBR(s)$. In the *refinement* step, for each pair that passes the filter step, the expensive intersection test on the exact object geometries is applied. To further reduce the number of pairs to be refined, *intermediate filters* can be added to the pipeline [10, 19, 56]. The main idea is to use, in addition to the MBR, object approximations that can help to identify fast whether a candidate pair (r, s) that passes the MBR filter is (i) a sure result, (ii) a sure non-result, or (iii) an indecisive pair, for which we still have to apply the geometry intersection test.

Previously proposed approximations in intermediate filters include simple convex polygons (5C or convex hull [10]), raster approximations [56], and "intervalized" raster approximations paired with binary codes [19]. Each of these approaches has its drawbacks. The convex polygons proposed in [10], although cheap to store and relatively fast to compute, can only be used to identify sure non-results and fail to reduce significantly the number of indecisive pairs that are sent to the expensive refinement step. The raster approximation technique of [56] occupies too much space and is not always effective in pruning object pairs. Finally, the state-of-the-art raster-intervals approach [19], which improves over [56] in terms of space complexity and pruning effectiveness, has a high preprocessing cost and occupies significant space.

In this paper, we propose APRIL (Approximating Polygons as Raster Interval Lists), a technique which significantly improves upon the Raster Intervals (RI) approach of [19], having the following key differences. First, previous rasterization techniques for spatial joins [19, 56] divide the raster cells that intersect a polygon in three classes: *Full* cells that are fully covered by the polygon, *Strong* cells that are covered by the polygon more than 50% but less than 100%, and *Weak* cells that are covered by the polygon by at most 50%. APRIL, *unites* Strong and Weak cell classes to a single *Partial* class, which simplifies storage and accelerates the intermediate filter.

Proceedings of the VLDB Endowment, Vol. 14, No. 1 ISSN 2150-8097.
doi:XX.XX/XXX.XX

Second, previous work [19, 56] explicitly stores or encodes cell-class information. The main novelty of APRIL is the representation of each object by two lists of intervals; one list that includes All cells (independently of their class) and one that includes only Full cells. The intermediate filter is then applied as a sequence of interval joins; All-All join (AA-join) filters out all non-results and then Full-All (FA-join), All-Full (AF-join) joins filter (i.e., identify) sure results, leaving indecisive pairs to the refinement step. Since there are no cell-specific comparisons, the intermediate filter using APRIL is much faster compared to RI [19] which performs comparisons at the cell level for each pair of intersecting intervals. Finally, APRIL applies a compression technique, based on delta encoding, to greatly reduce the space required to store the interval lists. This way, the APRIL approximations may require even less storage compared to object MBRs, making it possible to store and process them in the main memory. Moreover, APRIL's compression scheme allows partial, on-demand decompression of interval lists, which is conducted during interval join evaluation.

In addition to APRIL, the contributions of this paper include:

- We show the generality of APRIL in supporting spatial selection queries, spatial within joins, and joins between polygons and linestrings.
- We present a space partitioning approach, which increases the resolution of the raster grid and achieves more refined object approximations compared to [19] leading to fewer inconclusive cases and, therefore, faster query evaluation.
- We investigate options for defining and joining APRIL approximations of different polygons at different granularities based on their geometries.
- We propose a novel, one-step "intervalization" algorithm that computes the APRIL approximation of a polygon without having to rasterize it in full.

Our experimental evaluation on real data shows that, compared to the state-of-the-art intermediate filter (RI), APRIL is 3.5x-8.5x faster, (ii) occupies 2x-8x less space, and (iii) has orders of magnitude lower preprocessing cost. Using APRIL, the cost of end-to-end spatial join drops up to 71%, compared to using RI.

The rest of the paper is structured as follows: Section 2 provides the necessary background. Section 3 details APRIL's features, construction and usage. Section 4 offers customization options that help to further tune APRIL to fit the system's or dataset's needs. In Section 5 we study the efficient construction of APRIL approximations. Section 6 includes our experiments that verify APRIL's performance. Section 7 reviews related work and, finally, Section 8 concludes the paper with suggestions for future work.

2 BACKGROUND

The intersection join pipeline applies an MBR-join algorithm [9, 22, 47] on (indexed) MBR approximations of the objects, to identify pairs of object MBRs that intersect; these form *candidate* join results. The direct refinement of each candidate pair using computational geometry algorithms is very expensive and can easily take up to 99% of the end-to-end join cost [36]. In view of this, several studies [10, 19, 56] suggest the use of an *intermediate filter* based on more accurate object approximations than the MBR, to further reduce the number of object pairs that need to be refined. Figure 1 illustrates a general spatial intersection join pipeline that includes an intermediate filter. For each candidate join pair $(r.id, s.id)$ produced by the MBR-join, we perform a look-up of the *geometric approximations* (GAs) of objects r and s using their IDs, assuming a fast access method (e.g., $r.id$ is row-number in a table or vector storing R's GAs). The GAs are used by the intermediate filter to identify the pair $(r.id, s.id)$ as a true negative or a true hit, or forward it to the refinement step in order for it to access the exact geometries and make the ultimate decision (at a high computational cost).

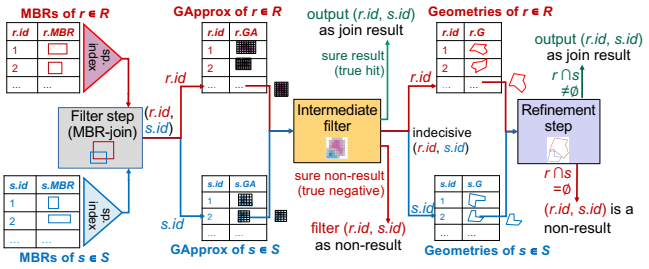

Figure 1: Spatial intersection join pipeline that includes an intermediate filter.

Raster Intervals (RI) [19] is the state-of-the-art intermediate filter. Assuming a global $2^N \times 2^N$ grid superimposed over the data space, RI approximates each object p by the set of cells in the grid that overlap p. Further, these cells are classified to *Full*, *Strong*, and *Weak*, based on their coverage percentage with the object's geometry (100%, $>$ 50% and $\leq$ 50%, respectively). Consider a candidate join pair of two objects r and s whose MBRs overlap. If there are no common cells in the approximations of r and s, then the pair is a true negative and is eliminated. If the objects have common cells, then it is possible to detect true hits by examining the types of common cells. All possible cases are shown in Table 1; if for at least one common cell its types in the two objects lead to a 'yes' case, then the object pair is a definite join result and the refinement step can be avoided. Figure 2 illustrates three cases of two polygonal objects, whose MBRs intersect. In Fig. 2(a), the two object approximations do not share any common cells, so the pair is pruned as a true negative. In Fig. 2(b), the two objects are reported as a join result (true hit); they definitely intersect because there exists a cell (the one with the bold-line border) which is fully covered by one of them and strongly covered by the other (see full-strong case in Table 1). In Fig. 2(c) all common cells in the two object approximations are either weak-weak or weak-strong, so the pair is determined as inconclusive and passed to the refinement step.

Table 1: Do two objects intersect, based on a common cell?

	weak	**strong**	**full**
weak	*inconclusive*	*inconclusive*	yes
strong	*inconclusive*	yes	yes
full	yes	yes	yes

To expedite the comparison of raster approximations of objects, RI maps each cell in the $2^N \times 2^N$ space to an integer in $[0, 2^{2N} - 1]$, which is the cell's order in the Hilbert space-filling curve [21]. Then, the cells in an object approximation with continuous IDs are merged into intervals $[start, end)$, which are sorted to form an *intervals list*. To capture the types of cells in each interval, the method uses

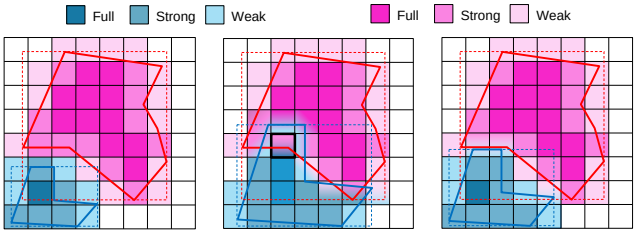

(a) true negative (b) true hit (c) inconclusive

Figure 2: Raster approximations as intermediate filters [56].

3-bit codes (Table 2), which are concatenated to form an interval's *coding*. The creation of Raster Intervals is illustrated in Figure 3.

The intermediate filter for a pair of objects is then implemented as follows. The sorted interval lists of the two objects are merged (as in merge-join) to identify pairs of intervals that overlap. For each such interval pair, the corresponding bit-codes are aligned and bitwise *AND*ed; if the result of an *AND* is non-zero then the object pair is immediately reported as a true hit; if there are no overlapping intervals, then the pair is reported as a true negative. If there is at least one pair of non-overlapping intervals and for all such pairs the bitwise *AND* of their codings is 0, then the pair is passed to the refinement step as indecisive.

Table 2: 3-bit type codes for each input dataset [19]

	input R	**input** S
full	011	101
strong	101	011
weak	100	010

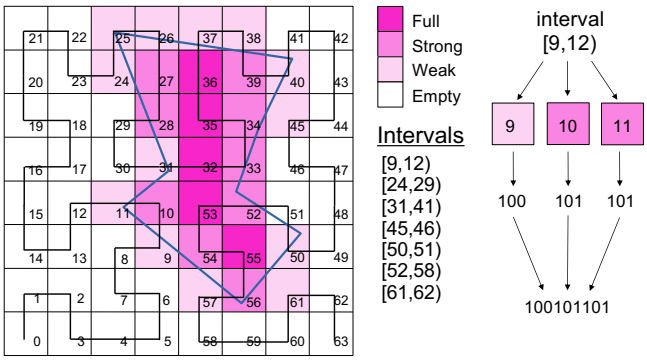

Figure 3: Hilbert curve cell enumeration and interval generation and encoding for a polygon in a 8×8 space [19].

In summary, the RI intermediate filter checks all common cells of two object approximations *en masse*. Even though RI offers high refinement candidate reduction compared to other polygon approximations, it comes with a number of drawbacks. First, the construction of RI approximations (i.e., pre-processing) is costly, because for each cell that overlaps with the object, we need to identify the cell type. Second, the intermediate filter involves a complex and relatively expensive bitstring alignment process. Third, RI approximations may occupy too much space, especially for large polygons that include long intervals with spacious encodings.

3 METHODOLOGY

We propose *APRIL* (Approximating Polygons as Raster Interval Lists), an enhanced intermediate filtering method for spatial intersection joins, which is more efficient and less space consuming compared to previous raster-based techniques [19, 56].

3.1 *A*- and *F*-Interval Lists

With APRIL, we reduce the approximation complexity of RI through two major changes. First, we unify the *Weak* and *Strong* cell types to a single cell type called *Partial*. Partial are non-empty cells which overlap with the polygon's area in less than 100% of their area; i.e., the cells that are intersected by the polygon's edges. Second, APRIL discards the bit-coding of RI; instead, each polygon is approximated simply by two sorted interval lists: the *A*-list and the *F*-list. The *A*-list is formed by intervals that concisely capture all cells that overlap with the polygon, regardless their type (Full or Partial), whereas the *F*-list captures only Full cells. An interval list having n intervals is stored as a simple sorted integer sequence in which the i-th interval's $start, end$ are located at positions $2i$ and $2i+1$ respectively, for $i \in [0, n)$.

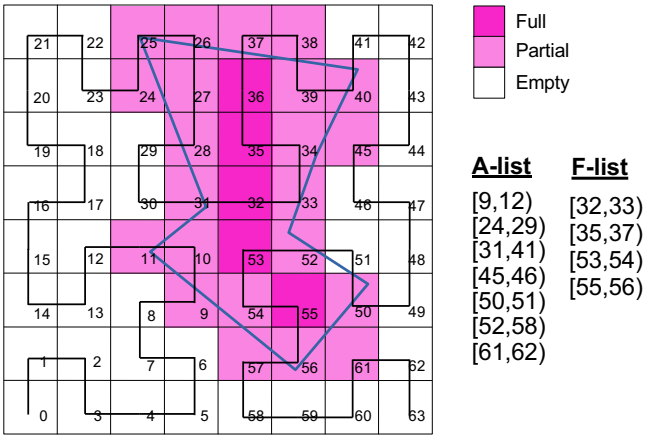

Figure 4: The interval generation for a polygon in a 8×8 space, without bit-coding and using interval lists.

The *A*-list and *F*-list for the example polygon of Figure 3 are shown in Figure 4. Strong and Weak cell types become Partial and the representation compared to RI is simplified. Note that the set of intervals in each of the *A*- and *F*- lists are disjoint. The new relationship identification table for a cell shared by two polygons, is shown in Table 3. Removing the Strong cell type renders the approximation unable to detect true hits for cells of the Strong-Strong case, as common cells that are both Partial cannot decide definite intersection between the two polygons.[1]

Construction To construct an APRIL approximation we need to first identify the cells intersected by the polygon's area in the grid, while also labeling each one of them as Partial or Full. Then, *Intervalization* derives the *F*-list, by sorting the set of Full cells by ID

[1] As we have found experimentally (Section 6), this has minimal effect on the amount of true hits and true negatives that the intermediate filter manages to detect. This is due to the fact that the only cases of true hits missed are pairs of polygons that intersect with each other *exclusively* in cells typed Strong for both polygons and nowhere else.

Table 3: APRIL: Do two objects intersect in a common cell?

	Partial	Full
Partial	*Inconclusive*	yes
Full	yes	yes

(i.e., Hilbert order) and merging consecutive cell IDs into intervals. To derive the A-list, we repeat this for the union of Full and Partial cells. In Section 5, we propose an efficient algorithm that derives the F- and A-list of a polygon without having to label each individual cell that intersects it.

3.2 APRIL Intermediate Spatial Join Filter

Similar to RI [19], APRIL is employed by an intermediate filter (Figure 1), between the MBR-filter and the refinement phase. Given a pair (r, s) of objects coming as a result of an MBR-join algorithm [11, 35, 47], APRIL uses the A- and F-lists of r and s to detect fast whether the polygons (i) are disjoint (true negative), (ii) are guaranteed to intersect (true hit), or (iii) are inconclusive, so they have to be forwarded to the refinement stage to verify their intersection.

Whether r and s are disjoint (i.e. do not intersect), can be determined by checking whether their A-lists have any pair overlapping of intervals or not. If they have no overlapping intervals, then r and s do not have any common cell in the grid and thus they cannot intersect. We check this condition by merge-joining the A-lists and stoping as soon as we detect two overlapping intervals.

Pairs of polygons that have at least one pair of overlapping intervals in their A-lists are then checked using their F-lists. We perform two more merge-joins: $A(r) \bowtie F(s)$ and $F(r) \bowtie A(s)$; detecting an overlapping intervals pair in one of these two joins means that there is a Full cell in one object that is common to a Full or Partial cell of the other object. This guarantees that the two objects intersect and the pair (r, s) is immediately reported as a spatial join result. If $A(r) \bowtie F(s)$ fails to detect (r, s) as a true hit, then $F(r) \bowtie A(s)$ is conducted; if the latter also fails, then (r, s) is an *inconclusive* candidate join pair, which is forwarded to the refinement step.

In summary, the APRIL intermediate filter sequence consists of 3 steps: the AA-join, AF-join, and FA-join, as illustrated in Figure 5 and described by Algorithm 1. Each step is a simple merge-join between two sorted interval lists. Since each list contains disjoint intervals, each of the three interval joins takes $O(n+m)$ time, where n and m are the lengths of the two interval join input lists. Hence, the total cost of the APRIL filter (i.e., Algorithm 1) is linear to the total number of intervals in the A- and F-lists of r and s.

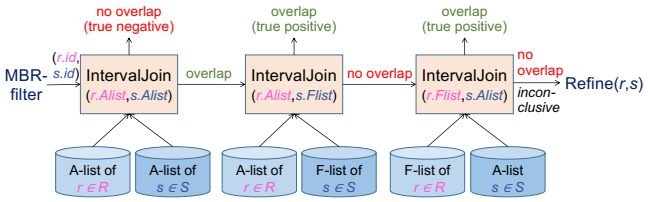

Figure 5: The 3 steps of the intermediate filter for a candidate pair of polygons.

Join Order Optimization The AA-join, AF-join, and FA-join could be applied in any order in Algorithm 1. For example, if (r, s) is a true hit, it would be more beneficial to perform the AF-join and the FA-join before the AA-join, as this would identify the hit earlier. On the other hand, if (r, s) is a true negative, conducting the AA-join first avoids the futile AF- and FA-joins. However, there is no way to know a priori whether (r, s) is a true hit or a true negative. In addition, we experimentally found that changing the join order does not have a high impact on the intermediate filter cost and the overall cost. For a typical candidate pair (r, s) the common cells are expected to be few compared to the total number of cells covered by either r or s, making AA-join the most reasonable join to start with. This is confirmed by our experiments where the number of candidate pairs identified as true negatives is typically much larger compared to the number of identified true hits.

Algorithm 1 APRIL join algorithm.

Require: (r, s) such that $MBR(r)$ intersects $MBR(s)$
1: **function** IntervalJoin(X, Y)
2: $i \leftarrow 0$; $j \leftarrow 0$
3: **while** $i < |X|$ and $j < |Y|$ **do**
4: **if** X_i overlaps with Y_j **then**
5: **return** *true* ▷ overlap exists
6: **end if**
7: **if** $X_i.end \leq Y_j.end$ **then** $i \leftarrow i + 1$ **else** $j \leftarrow j + 1$
8: **end while**
9: **return** *false* ▷ no overlaps detected
10: **end function**
11:
12: **if** not IntervalJoin($A(r), A(s)$) **then**
13: **return** *false* ▷ true negative
14: **end if**
15: **if** IntervalJoin($A(r), F(s)$) **then**
16: **return** *true* ▷ true hit
17: **end if**
18: **if** IntervalJoin($F(r), A(s)$) **then**
19: **return** *true* ▷ true hit
20: **end if**
21: **return** REFINEMENT(r, s) ▷ forward pair to refinement

3.3 Generality

In this section, we demonstrate the generality of APRIL in supporting other queries besides spatial intersection joins between polygon-sets. We first show how we can use it as an intermediate filter in selection (range) queries. Then, we discuss its application in spatial *within* joins. Finally, we discuss the potential of using APRIL approximations of polygons and raster approximation of linestrings to filter pairs in polygon-linestring intersection joins.

3.3.1 Selection Queries. Similarly to joins, APRIL can be used in an intermediate filter to reduce the cost of selection queries. Consider a spatial database system, which manages polygons and where the user can draw a selection query as arbitrary polygon QP; the objective is to retrieve the data polygons that intersect with the query polygon QP. Assuming that we have pre-processed all data polygons and computed and stored their APRIL representations, we can process polygonal selection queries as follows. We first pre-process QP to create its APRIL approximation. Then, we use the MBR of QP to find fast the data polygons whose MBR intersects with the MBR of the query (potentially with the help of an index [20, 48]). For each such data polygon r, we apply the APRIL intermediate filter for the (r, QP) pair to find fast whether r is a true negative or a true hit. If r cannot be pruned or confirmed as a query result, we eventually apply the refinement step.

3.3.2 Spatial Within Joins. APRIL can also applied for spatial joins having a *within* predicate, where the objective is to find the pairs (r, s), where $r \in R$ and $s \in S$ and r is *within* s (i.e., r is completely covered by s). In this case, the intermediate filter performs only 2 of its 3 steps. The *AA*-join is applied first to detect whether r and s are disjoint, in which case the pair should be eliminated. Then, we perform a variant of the *AF*-join, where the objective is to find if *every* interval in the *A*-list of r is contained in one interval in the *F*-list of s; if this is true, then (r, s) is guaranteed to be a within join result and it is reported as a true hit. In the opposite case, (r, s) is forwarded to the refinement step. We do not apply an *FA*-join, because this may only detect whether s is within r.

3.3.3 Linestring to Polygon Joins. Another interesting question is whether APRIL can be useful for intersection joins between other spatial data types, besides polygons. The direct answer is no, since APRIL is designed for voluminous objects. Still, our method can be useful for the case of joins between polygons and linestrings. A linestring is a sequence of line segments and it is used to approximate geographic objects such as roads and rivers. The rasterization of a linestring only gives Partial cells, as linestrings do not have volume and may not cover a cell entirely. In addition, as exemplified in Figure 6, linestrings do not really benefit from merging consecutive cells into intervals, as linestrings that follow the Hilbert order (or any other fixed space-filling curve) are rare. Hence, it is more space-efficient to approximate a linestring as a sorted sequence of cell-IDs (which are guaranteed to be Partial). Having the linestring approximations, we can evaluate spatial intersection joins between a collection of polygons and a collection of linestrings, by applying 2 of the 3 steps in the APRIL intermediate filter; namely, (i) a merge-join between the *A*-list of the polygon and the cell-ID list of the linestring to find out whether the pair is a true negative and (ii) a merge-join between the *F*-list of the polygon and the cell-ID list of the linestring to find out whether the pair is a true hit. Algorithm 1 can easily be adapted for polygon-linestring filtering, by simply changing IntervalJoin(X, Y) to take a sequence of cell-IDs Y as treat them as intervals of duration 1.

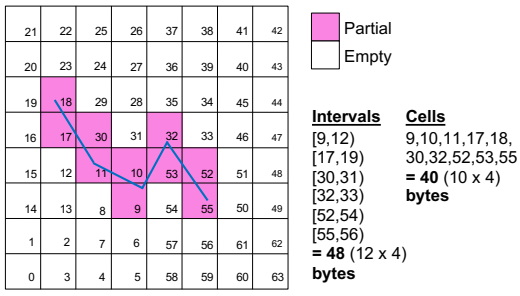

Figure 6: A linestring's APRIL approximation size in bytes, if stored as intervals versus cells.

4 CUSTOMIZATION

We have explored a series of optimization and customization options that can potentially reduce APRIL's space complexity and improve its performance in terms of filter effectiveness and speed.

4.1 Compression

Recall that the only information that APRIL stores for each polygon is two interval lists: the *A*-list and the *F*-list. The interval lists are essentially sorted integer arrays, so we can exploit delta encoding and more specialized lossless compression schemes to reduce their space requirements. Since any of the *AA*- *AF*- and *FA*-join that we may apply on the lists may terminate early (as soon as an interval overlap is detected), we should go for a compression scheme that does not require the decompression a list entirely before starting processing it. In other words, we should be able to perform joins *while* decompressing the lists. This way, we may avoid uncompressing the lists at their entirety and still be able to perform the joins. In view of this, we use delta encoding, where we store the first value of the list precisely and from thereon store the differences (gaps) between consecutive numbers.

There are dozens of different compression schemes for gaps between ordered integers, each with their pros and cons. We chose the Variable Byte (VByte) method [13, 46], a popular technique that even though it rarely achieves optimal compression, it is adequately efficient and really fast [24]. We use the libvbyte [12] library that has an option for sorted integer list compression, which matches our case and boosts performance by utilizing delta encoding.

At the same time, we adapt our interval join algorithm to apply decompression and join at the same time, i.e., each time it needs to get the next integer from the list it decompresses its value and adds it to the previous value in the list.

4.2 Partitioning

The accuracy of APRIL as a filter is intertwined with the grid granularity we choose. A more fine-grained grid results in more Full cells, increasing the chance of detecting true hits; similarly, empty cells increase, enhancing true negative detection. However, simply raising the order N is not enough to improve performance. Increasing N beyond 16 means that a single unsigned integer is not enough to store a Hilbert curve's identifier, which range from $[0, 2^{2N} - 1]$. For $N = 17$ or higher, we would need 8 bytes (i.e., an unsigned long) to store each interval endpoint, exploding the space requirements and the access/processing cost.

In view of this, we introduce a partitioning mechanism for APRIL, that divides the data space into *disjoint* partitions and defines a dedicated rasterization grid and Hilbert curve of order $N = 16$ to each partition. This increases the global granularity of the approximation, without using long integers, while giving us the opportunity to define smaller partitions for denser areas of the map for which a finer granularity is more beneficial. Partitioning is done considering all datasets/layers of the map. That is, the same space partitioning is used for all datasets that are joined together. The contents of each partition are all objects that intersect it; hence, the *raster* area of the partition is defined by the MBR of these objects and may be larger than the partition, as shown in the example of Figure 7. APRIL approximations are defined based on the raster area of the partition. The spatial join is then decomposed to multiple joins, one for each spatial partition. Duplicate join results are avoided at the filter step of the join (MBR-join) as shown in [14, 47] .

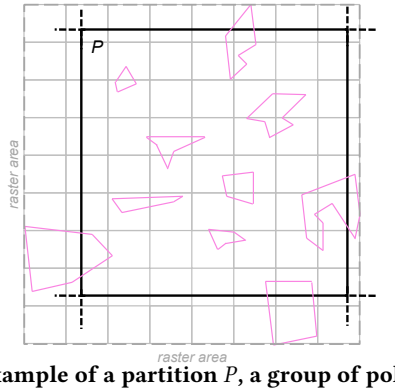

Figure 7: Example of a partition P, a group of polygons in it and P's raster area with granularity order $N = 8$.

4.3 Different Granularity

If we use the same (fine) grid to rasterize all polygons, the APRIL approximations of large polygons may contain too many intervals, slowing down the intermediate filter. We can create approximations using a different order N of the Hilbert curve for different datasets, based on the average sizes of their contents. There is a trade-off between memory and performance, since an order lower than 16 means fewer intervals and thus lower memory requirements and complexity, but also means reduced APRIL accuracy.

When joining two APRIL approximations of different order, we need to adjust one of the two interval lists so that it can be joined with the other. For this, we scale down the list with the highest order. Specifically, before comparing two intervals $a = [a_{start}, a_{end})$ and $b = [b_{start}, b_{end})$ at orders N and L respectively, where $N > L$, the highest order interval a should be right shifted by $n = |N - L| \times 2$ bits, to form a transformed interval a', as follows:

$$a' = [a_{start} >> n, (a_{end} - 1) >> n] \quad (1)$$

Right shifting creates intervals in a more coarse-grained grid and thus, they may represent larger areas than the original. Therefore, this formula works only for A-intervals, since there is no guarantee that a Full interval at order N will also be Full at order L. For this reason, in Algorithm 1, we perform only one of the AF- and FA-joins, using the F-list of the coarse approximation (which is not scaled down). This has a negative effect on the filter's effectiveness, as a trade-off for the coarser (and smaller) APRIL approximations that we may use for large polygons.

5 APRIL APPROXIMATION CONSTRUCTION

In this section, we present two methods for the construction of a polygon's APRIL approximation. In Section 5.1 we present a *rasterization* approach that efficiently finds the cells that intersect an input polygon and their types, based on previous research on polygon rasterization, and then sorts them to construct the A- and F-interval lists. In Section 5.2, we propose a more efficient approach tailored for APRIL, which avoids classifying all cells, but directly identifies the intervals and constructs the A- and F-interval lists.

5.1 Efficient Graphics-Inspired Rasterization

Previous raster-based filters [19, 56] require the classification of each cell to Full, Strong, Weak, or Empty, based on the percentage of the cell covered by the original polygonal geometry. For this, they apply an algorithm that involves numerous polygon clippings and polygonal area computations, at a high cost. On the other hand, to define a APRIL approximation, we only need to identify the cells which are partially or fully covered by the input polygon's area. Inspired by rasterization techniques in the graphics community, we propose a polygon rasterization technique which involves two stages. Firstly, we compute the Partial cells, which essentially form the boundary of the polygon in the grid. Next, we compute the Full cells using the previously-computed boundary cells.

Identifying the Partial cells is closely related to the pixel drawing problem in graphics that involves detecting which cells to "turn on" to draw a target line. While Bresenham's algorithm [8] is a popular and fast pixel drawing algorithm, it approximates a line segment by turning on a minimal amount of cells and may thus not detect all intersected cells. In contrast, the Digital Differential Analyzer (DDA) method [28] is slower, but identifies correctly and completely all intersected cells. To detect the Partial cells, we use an efficient variant of DDA [4] that uses grid traversal. We execute the grid traversal for each edge of the polygon and store the IDs of the identified Partial cells in a list. The leftmost grid in Figure 8 shows the Partial cells detected by the grid traversal algorithm for the polygon drawn in the figure.

Next, to identify the Full cells, a naive approach would be to sweep the grid in each line, starting from the polygon's leftmost Partial cell, and "fill" the grid until reaching another Partial cell. Instead, we use a more efficient technique, called *flood fill* [39], which is commonly used to color or "fill" a closed area in an image. The classic flood fill algorithm first selects an unlabeled cell that is guaranteed to be within the polygon, called *seed*. Then, it traverses all neighboring cells of the seed until it finds the boundaries of the closed area, classifying the encountered cells as fully covered. We implemented a variant of this algorithm which minimizes the number of point-in-polygon tests required to identify whether a cell is inside or outside the polygon. Specifically, we iterate through the cells of the polygon's MBR area. If a cell c has not been labeled yet (e.g., as Partial), we perform a point-in-polygon check from c's center. If the cell c is found to be inside the polygon, c is marked as Full and we perform a flood fill using c as the seed, stopping at labeled cells, and label all encountered unchecked cells as Full. If the cell c is found to be outside the polygon, c is marked as Empty and we perform flood fill to mark Empty cells. The algorithm repeats as long as there are unchecked cells to flood fill from. This reduces the number of point-in-polygon tests that need to be performed, as it suffices to perform a single test for each contiguous region in the grid with Full or Empty cells.

Figure 8 illustrates the complete flood fill process for an example polygon. The unchecked cells form three contiguous regions bounded by Partial cells, two of them being outside the polygon and one inside. Instead of looking for cells within the polygon to flood fill starting from them, it is faster to fill both the inside and outside of the polygon (marking cells as Full and Empty, respectively), as the number of point-in-polygon tests is minimized.

After all Partial and Full cells have been identified, the algorithm merges consecutive cell identifiers into intervals to create the A- and F-lists that form the APRIL approximation.

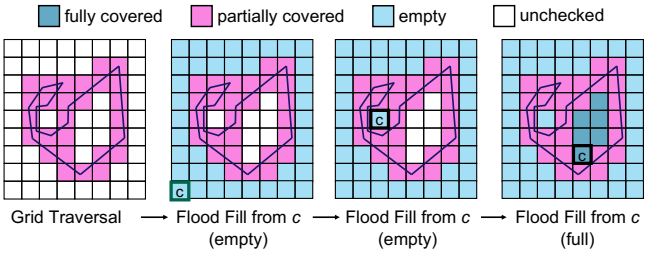

Figure 8: The flood fill algorithm, performing 3 iterations with different seeds c to completely fill all unchecked cells.

5.2 One-Step Intervalization

The approach described in the previous section identifies the types (Partial, Full, Empty) of all cells that intersect the MBR of the input polygon. For polygons which are relatively large and their MBRs define a large raster area this can be quite expensive. We propose an alternative approach that identifies the F-intervals of the APRIL approximation efficiently and directly uses them to identify the A-intervals that include them in one step, without the need to identify the types of all individual cells in them.

As in Section 5.1, we first apply DDA [4] to detect the Partial cells and sort them in Hilbert order. An important observation is that "gaps" between nonconsecutive identifiers in the sorted Partial cells list, indicate candidate Full intervals on the Hilbert curve. Figure 9 illustrates how these gaps are formed for an example polygon. Identifying the first cell c of each candidate interval as Full or Empty, through a point-in-polygon (PiP) test, is enough to label the whole interval as Full or Empty, respectively. In the figure, the first "gap" interval is $[7, 8)$ containing just cell 7, which can be marked empty after a PiP test. From all "gap" intervals those marked in **bold** (i.e., 32-34 = $[32, 35)$ and 52-54 = $[52, 55)$) are Full intervals and can be identified as such by a PiP test at their first cell (i.e., 32 and 52, respectively).

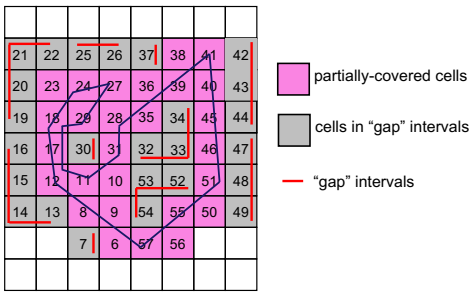

[6,7,8,9,10,11,12,13-16,17,18,19-22,23,24,25-26,27,28,29,30,31,
32-34,35,36,37,38,39,40,41,42-44,45,46,47-49,50,51,**52-54**,55,56,57]

Figure 9: Example of the intervals/gaps for a set of Partial cells. Whether a gap will be labeled as Full or Empty, depends on the outcome of the PiP test.

Additionally, we can skip some of these PiP tests by checking all adjacent cells (north, south, west, east) of the first cell c with smaller identifiers than c; if any of them is Full or Empty, we can also give the same label to the candidate interval, as it should exist in the same inner/outer area of the raster image. For example, in Figure 9, when the algorithm moves to identify the interval $[52, 55)$, it can detect that its first cell 52 is adjacent to another Full cell with smaller order (cell 33), that has been previously identified. Thus, the interval $[52, 55)$ exists in the same inner area as cell 33 and it inherits its label (Full), without performing another PiP test for it. In this example, a total of 5 PiP tests will be performed, for the intervals that start with the cells 7, 13, 30, 32 and 42, instead of 11 PiP tests that would be performed otherwise, if we did not take into consideration the neighboring cells.

Algorithm 2 is a pseudocode for the one-step intervalization process, which takes as input the sorted Partial cells list P computed by DDA. The algorithm creates the A-list, F-list of the polygon in a single loop through P. In a nutshell, the algorithm keeps track of the starting point of every A-interval and when an empty gap is identified, the algorithm "closes" the current A-interval and starts the next one from the next Partial cell in the list. On the other hand, Full intervals start with the identifier of the cell that is right after the last Partial cell of a consecutive sequence and end before the next Partial cell in order.

In details, Algorithm 2, starting from the first cell p in P, keeps track of the starting cell-ID $Astart$ of the current A-interval; while the next cell $p+1$ in Hilbert order is also in P (Lines 3–9) the current A-interval is expanded. If the next cell $c = p + 1$ is not partial, it is the starting cell of a candidate F-interval. We first apply function $CheckNeighbors(c)$ to find whether there exists an adjacent cell of c which is part of a $FULL$ or $EMPTY$ interval. Specifically, for cell c and a neighbor n, we first check whether $n < c$ (if not, n is either Partial or unchecked); if yes, we binary-search P to check whether n is a P-cell. If not, we apply a special binary search method on the current F-list to find out whether n is part of an interval in it. If we find n as part of an F-interval, then c is definitely a Full cell. If we do no find n, then c is definitely an Empty cell because $n < c$ and n is not Partial. If for all neighbors n of c, either $n > c$ or n is Partial, then we cannot determine the type of c based on the current data, so we perform a PiP test to determine c's type (i.e., Full or Empty). If c is Full, then we know that the entire interval $[c, p)$ is $FULL$ and append it to the F-list (Line 16). Otherwise (c is Empty), c is the end of the current A-interval, so the interval is added to the A-list and the start of the next A-interval is set to the next Partial cell p. The algorithm continues until the list P of partial cells is exhausted and commits the last A-interval (Line 23).

Our one-step intervalization approach performs $|P| - 1$ PiP tests in the worst-case, which dominate its cost. Compared to the FloodFill-based approach of Section 5.1, which explicitly marks and then sorts all Full and Partial cells, Algorithm 2 is expected to be much faster for polygons which are large compared to the cell size and include a huge number of Full cells. On the other hand, flood filling may be a better fit for small polygons with a small MBR and relatively few Full cells.

6 EXPERIMENTAL ANALYSIS

We assess the performance of our proposed APRIL method, by experimentally comparing it with previously proposed polygon approximations for intermediate filtering of spatial joins. These include the combined use of 5-Corner and Convex Hull (5C+CH)

Table 4: Statistics of the datasets and space requirements of the data and the approximations

	T1	T2	T3	O5AF	O6AF	O5AS	O6AS	O5EU	O6EU	O5NA	O6NA	O5SA	O6SA	O5OC	O6OC
# of Polygons	123K	2.25M	3.1K	72K	191K	447K	622K	1.9M	7.1M	4.0M	999K	123K	228K	107K	223K
Avg # of vertices	25.4	31.9	2285.0	58.9	36.3	45.3	41.9	35.1	32.1	37.6	47.5	47.5	41.6	48.4	42.7
Avg obj MBR area	1.77E-04	4.03E-05	3.95E-01	2.03E-03	1.23E-03	1.03E-03	9.98E-04	1.25E-04	1.19E-04	1.11E-04	4.40E-04	1.34E-03	2.37E-03	5.00E-04	5.27E-04
Geometries size (MB)	51.1	1168.1	115.3	68.9	112.7	327.9	422.1	1120.7	3746.2	2453.4	767.4	94.9	153.7	84.2	151.3
MBR size (MB)	4.4	81.1	0.1	2.6	6.9	16.1	22.4	70.9	258.4	144.8	36.0	4.5	8.2	3.9	8.1
APRIL size (MB)	14.4	134.0	57.2	14.2	25.4	55.2	64.5	180.3	968.0	251.0	155.0	25.4	44.4	7.3	15.0
APRIL-C size (MB)	6.6	75.3	16.0	5.1	10.6	23.3	28.6	84.8	406.5	138.0	62.4	9.2	16.7	3.8	7.8
RI size (MB)	19.5	138.2	968.7	18.6	55.7	57.5	109.8	180.9	942.9	238.1	213.5	31.2	143.4	14.2	39.3
RA size (MB)	1100.0	20000.0	N/A	617.2	1700.0	3700.0	5700.0	342.2	11400.0	6200.0	1500.0	1100.0	2100.0	898.7	2000.0
5C-CH size (MB)	28.7	705.4	1.6	18.5	46.6	117.8	159.4	515.4	1700.0	1200.0	257.7	30.4	52.9	28.8	57.7

Algorithm 2 The One-Step Intervalization algorithm.

Require: Sorted Partial cell array P
1: **function** OneStepIntervalization(P)
2: $i \leftarrow 0$ ▷ current position in array P
3: $Astart \leftarrow P_i; p \leftarrow P_i$ ▷ cell-IDs of current A-interval and partial cell
4: **while** $i < |P|$ and $p + 1 = P_{i+1}$ **do** ▷ while next cell is partial
5: $i \leftarrow i + 1$
6: $p \leftarrow P_i$
7: **end while**
8: $c \leftarrow p + 1$ ▷ next uncertain cell
9: $i \leftarrow i + 1; p \leftarrow P_i$ ▷ next partial cell
10: **while** $i < |P|$ **do**
11: $type \leftarrow CheckNeighbors(c)$
12: **if** $type \neq FULL$ and $type \neq EMPTY$ **then** ▷ $type$ is still uncertain
13: $type \leftarrow PointInPolygon(c)$ ▷ PiP test gives $FULL$ or $EMPTY$
14: **end if**
15: **if** $type = FULL$ **then**
16: $AppendFullInterval([c, p))$
17: **else** ▷ $type$ is $EMPTY$
18: $AppendAllInterval([Astart, c))$ ▷ current A-interval finalized
19: $Astart \leftarrow p$ ▷ start new A-interval
20: **end if**
21: Execute Lines 3–9 ▷ go through partial cells until next gap
22: **end while**
23: $AppendAllInterval([Astart, P_{i-1} + 1))$ ▷ save last ALL interval
24: **end function**

(as proposed in [10]), Raster Approximation (RA) [56], and the state-of-the-art Raster Intervals (RI) [19]. We also included a baseline approach (None), which does not apply an intermediate filter between the MBR-join and the refinement step. For RA, we set the grid resolution to $K = 750$ cells, except for a few datasets where we use $K = 100$, due to memory constraints. The MBR filter of the spatial join pipeline was implemented using the algorithm of [47]. The refinement step was implemented using the Boost Geometry library [7] and its functions regarding shape intersection. All code was written in C++ and compiled with the -O3 flag. The experiments were run on a machine with a 3.6GHz Intel i9-10850k and 32GB RAM, running Linux.

6.1 Datasets

We used datasets from SpatialHadoop's [40] collection. T1, T2, and T3 represent landmark, water and county areas in the United States (conterminous states only). We also used two Open Street Maps (OSM) datasets (O5 and O6) that contain lakes and parks, respectively, from all around the globe. We grouped objects into continents and created 6 smaller datasets representing each one: Africa (O5AF, O6AF), Asia (O5AS, O6AS), Europe (O5EU, O6EU), North America (O5NA, O6NA), Oceania (O5OC, O6OC) and South America (O5SA, O6SA). From all datasets, we removed any non-polygonal objects as well as multi-polygons and self-intersecting polygons. The first three rows of Table 4 show statistics about the datasets. We conducted spatial joins only between pairs of datasets that cover the same area (i.e., T1 ⋈ T2, T1 ⋈ T3, O5AF ⋈ O6AF, etc.).

6.2 Comparative Study

In the first set of experiments, we compare APRIL with other intermediate filters in terms of space complexity, filter effectiveness, and filter cost. For all experiments, we created APRIL and RI using a single partition (i.e., the map of the two datasets that are joined in each case), rasterized on a $2^{16} \times 2^{16}$ grid. We used a fixed order (*AA*-, *AF*-, *FA*-) for the interval joins of APRIL, as shown in Algorithm 1.

6.2.1 Space Complexity. Table 4 shows the total space requirements of the object approximations required by each intermediate filter, for each of the datasets used in our experiments. APRIL and APRIL-C refer to the uncompressed and compressed version of APRIL, respectively. As a basis of comparison we also show the total space required to store the exact geometries of the objects and their MBRs. In most cases, APRIL has the lowest space requirements compared to all other filters. Notably, for most datasets, the compressed APRIL approximations have similar space requirements as the object MBRs, meaning that we can keep them in memory and use them in main-memory spatial joins [29] directly after the MBR-join step, without incurring any I/O.

6.2.2 Performance in Spatial Intersection Joins. We evaluate APRIL (both compressed and uncompressed version), 5C+CH, RA, and RI, on all join pairs, in Figure 10. We compare their ability to detect true hits and true negatives, their computational costs as filters, and their impact to the end-to-end cost of the spatial join.

Filter Effectiveness APRIL and RI have the highest filter effectiveness among all approximations across the board. APRIL's true hit ratio is slightly smaller compared to that of RI because APRIL fails to detect the (rare) pairs of polygons which only have Strong-Strong common cells. However, this only brings a marginal increase in the refinement step's cost, at the benefit of having a faster and more space-efficient filter. In O5AS ⋈ O6AS and O5OC ⋈ O6OC, APRIL and RI have marginally lower true hit ratio compared to RA; however, in these cases their true negative ratio is much higher than that of RA. The least effective filter is 5C+CH, mainly due to its inability to detect true hits.

Intermediate Filter cost 5C+CH are simple approximations (a few points each), therefore the corresponding filter is very fast to apply. Hence, 5C+CH has the lowest cost for most joins. Notably, APRIL has a filtering cost very close to that of 5C+CH and sometimes even

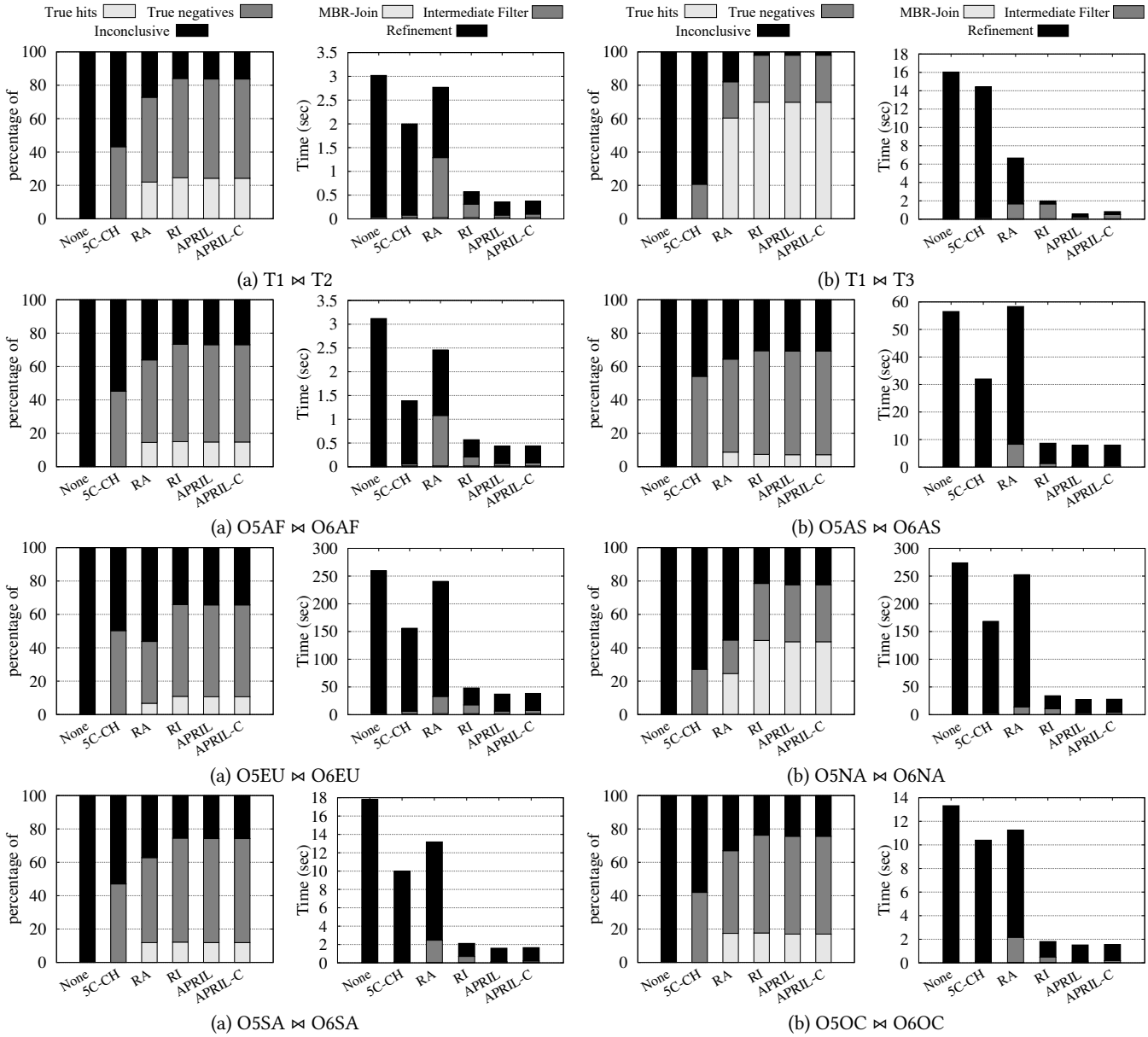

Figure 10: Filter effectiveness and spatial join cost for various intermediate filters.

lower. This is due to APRIL's ability to model a raster approximation as two sequences of integers, which are processed by a sequence of efficient merge-join algorithms. On the other hand, the application of the RI filter is more expensive because, besides the interval join, it requires the alignment and bitwise *AND*ing of the interval bit-codes. As a result, APRIL is 3.5-8.5 times faster as an intermediate filter compared to RI. Even though 5C+CH is the fastest filter to apply, it has poor filtering performance, which negatively affects the total join cost (last column), whereas APRIL is very fast and very effective at the same time. A comparison between the filter costs of APRIL and APRIL-C reveals that decompressing the interval lists while performing the joins in APRIL-C only brings a small overhead, making compression well worthy, considering the significant space savings it offers (see Table 4). The decompression cost is significant only in T1 ⋈ T3, because T3's *A*-lists and *F*-lists are quite long. Still, even in this case, APRIL-C is much faster than RI.

Refinement cost The refinement cost is intertwined with the percentage if indecisive pairs. The detection of fewer candidate pairs as true hits or true negatives leads to a higher refinement workload; this is why APRIL and RI result in the lowest refinement cost, compared to the rest of the approximations.

Overall cost APRIL reduces the overall cost of end-to-end spatial joins up to 3 times compared to the state-of-the-art RI intermediate filter, while also achieving a speedup of 3.23x-25x against the rest of

Table 5: APRIL vs. RI (polygonal range queries).

	True hits	True negatives	Indecisive	Int. Filter (s)	Refinement (s)	Total (s)
	1000 T3 queries against T1					
RI	**69.28%**	28.60%	**2.12%**	0.52	0.10	0.64
APRIL	69.27%	28.60%	2.13%	**0.06**	0.10	**0.18**
	1000 T3 queries against T2					
RI	68.46%	29.87%	1.67%	9.26	1.58	11.07
APRIL	68.46%	29.87%	1.67%	**1.02**	1.58	**2.84**

Table 6: Performance of filters (spatial within joins)

	True hits	True negatives	Indecisive	Int. Filter (s)	Refinement (s)	Total (s)
	T2 ⋈ T1 (Tiger water in landmark areas)					
None	0.00%	0.00%	100.00%	0.00	3.61	3.64
5C+CH	0.00%	34.71%	65.29%	0.10	1.33	1.46
RA	13.48%	29.18%	57.34%	0.14	1.11	1.28
RI	**18.48%**	**59.46%**	**22.06%**	0.20	**0.48**	0.71
APRIL	**18.48%**	59.42%	22.11%	**0.05**	0.49	**0.58**
	T1 ⋈ T3 (Tiger landmark in county areas)					
None	0.00%	0.00%	100.00%	0.00	20.14	20.19
5C+CH	0.00%	20.72%	79.28%	0.37	14.02	14.44
RA	44.35%	14.29%	41.36%	0.51	8.26	8.82
RI	**68.05%**	**28.13%**	**3.82%**	1.56	**0.80**	2.41
APRIL	**68.05%**	**28.13%**	**3.82%**	**0.21**	**0.80**	**1.06**
	T2 ⋈ T3 (Tiger water in county areas)					
None	0.00%	0.00%	100.00%	0.00	383.49	384.23
5C+CH	0.00%	22.17%	77.83%	7.70	274.54	282.98
RA	42.50%	15.25%	42.25%	9.53	165.50	175.77
RI	**67.36%**	**29.88%**	**2.75%**	27.08	**12.22**	40.04
APRIL	**67.36%**	**29.88%**	**2.75%**	**3.47**	**12.22**	**16.43**

the approximations. Adding the APRIL intermediate filter between the MBR-filter and the refinement step reduces the spatial join cost by 7x-28x. APRIL's high filtering effectiveness, low application cost, and low memory requirements render it a superior approximation for filtering pairs in spatial intersection join pipelines.

6.2.3 Performance in other queries. Next, we evaluate the performance of APRIL in other queries, besides spatial intersection joins. We start with selection queries of arbitrary shape (see Section 3.3.1). For this experiment, we sampled 1000 polygons from T3 and applied them as selection queries on T1 and T2, simulating queries of the form: find all landmark areas (T1) or water areas (T2) that intersect with a given US county (T3). As Table 5 shows, compared to RI, APRIL achieves a 3.5x-4x speedup in the total query cost.

Next, we compare all methods in spatial *within* joins, where the objective is to find pairs (r, s) such that r is within s (see Section 3.3.2). As Table 6 shows, APRIL again achieves the best performance, due to its extremely low filtering cost. APRIL is even faster than 5C+CH, because 5C+CH performs two polygon-in-polygon tests which are slower compared to a polygon intersection test.

Finally, we test the effectiveness of APRIL in polygon-linestring joins, as described in Section 3.3.3. For this experiment, we join the polygon sets T1, T2, and T3 with dataset T8 (from the same collection), which contains 16.9M linestrings (roads in the United States), each having 20.4 vertices on average. In this comparison, we do not include RI and RA, because Strong cell types cannot be used to detect true hits. Table 7 compares APRIL with 5C+CH and the skipping of an intermediate filter (None). 5C+CH only detects true negatives (in the case where the 5C+CH approximations do not intersect). APRIL outperforms 5C+CH by at least three times in total join time and by orders of magnitude in T3 ⋈ T8, where it can identify the great majority of join results as true hits.

Table 7: Polygon-linestring spatial intersection joins.

	True hits	True negatives	Indecisive	Int. Filter (s)	Refinement (s)	Total (s)
	T1 ⋈ T8 (Tiger landmarks and roads)					
None	0.00%	0.00%	100.00%	0.00	27.82	28.25
5C+CH	0.00%	45.24%	54.76%	1.07	15.99	17.49
APRIL	**12.70%**	**55.01%**	**32.29%**	**0.93**	**3.82**	**5.18**
	T2 ⋈ T8 (Tiger water areas and roads)					
None	0.00%	0.00%	100.00%	0.00	238.91	241.59
5C+CH	0.00%	68.13%	31.87%	6.24	90.60	99.52
APRIL	**0.08%**	**90.22%**	**9.71%**	**5.58**	**19.92**	**28.17**
	T3 ⋈ T8 (Tiger county areas and roads)					
None	0.00%	0.00%	100.00%	0.00	2546.48	2543.37
5C+CH	0.00%	22.79%	77.21%	16.21	1855.63	1878.73
APRIL	**66.25%**	**30.77%**	**2.98%**	**25.64**	**58.23**	**90.77**

Table 8: Join order effect on APRIL filter cost.

Join Order	True hits	True negatives	Indecisive	Int. Filter (s)
	T1 ⋈ T2			
AA-AF-FA	24.29%	59.42%	16.29%	0.0505
AA-FA-AF	24.29%	59.42%	16.29%	**0.0501**
AF-FA-AA	24.29%	59.42%	16.29%	0.0585
FA-AF-AA	24.29%	59.42%	16.29%	0.0601
	T1 ⋈ T3			
AA-AF-FA	69.84%	28.13%	2.03%	0.1872
AA-FA-AF	69.84%	28.13%	2.03%	0.1891
AF-FA-AA	69.84%	28.13%	2.03%	**0.1737**
FA-AF-AA	69.84%	28.13%	2.03%	0.1773

6.3 Optimizations and Customizations

6.3.1 Join Order. So far the interval joins in APRIL have been applied in a fixed order: *AA*, *AF*, and *FA*. As discussed in Section 3.2, the joins can be performed in any order. Table 8 tests different join orders for T1 ⋈ T2 and T1 ⋈ T3. T1 ⋈ T2 (like the majority of tested joins) has a high percentage of true negatives, so the original order is the most efficient one (changing the order of *AF* and *FA* does not make a difference). On the other hand, for T1 ⋈ T3, where the true hits are more, pushing the *AA*-join at the end is more beneficial. Since knowing the number (or probability) of true negatives and true hits a priori is impossible and because the join order does not make a big difference in the efficiency of the filter (especially to the end-to-end join time), we suggest using the fixed order, which is the best one in most tested cases. In the future, we investigate the use of data statistics and/or object MBRs to fast guess a good join order on an object pair basis.

6.3.2 Partitioning. Tables 9 and 10 illustrate the effect of data partitioning (Section 4.2) on the effectiveness, query evaluation time, and space requirements of APRIL approximations. A higher number of partitions means finer-grained grids per partition and thus, more intervals per polygon (i.e., more space is required). Even though this reduces the amount of inconclusive cases, it can slow down the intermediate filter, since more intervals need to be traversed per candidate pair. For example, T1 ⋈ T3 has already a small percentage of inconclusive pairs, so partitioning may not bring a significant reduction in the total join time. On the other hand, for joins with high inconclusive percentage, such as O5AS ⋈ O6AS, partitioning can greatly reduce the total cost. In summary, partitioning comes with a time/space tradeoff.

6.3.3 Different Granularity. As discussed in Section 4.3, we can define and use APRIL at lower granularity than $N = 16$ for one or both datasets, trading filter effectiveness for space savings. In Table 11, we study the effect of reducing N for T3 in T1 ⋈ T3. The size of T3's APRIL approximations halves every time we decrease N by

Table 9: # partitions per dimension effect on join time.

#	Indecisive	Int. Filter (s)	Refinement (s)	Total time (s)
	T1 ⋈ T2			
1	16.29%	0.08	0.27	0.39
2	12.81%	0.06	0.22	0.32
3	11.36%	0.08	0.20	**0.30**
4	10.50%	0.09	0.20	0.32
	T1 ⋈ T3			
1	2.03%	0.47	0.34	0.86
2	1.77%	0.29	0.29	**0.62**
3	1.67%	0.37	0.27	0.69
4	1.64%	0.49	0.26	0.80
	O5AF ⋈ O6AF			
1	26.92%	0.06	0.36	0.45
2	21.24%	0.06	0.29	0.37
3	18.26%	0.07	0.25	**0.34**
4	16.63%	0.08	0.24	0.35
	O5AS ⋈ O6AS			
1	30.76%	0.43	7.48	8.04
2	24.07%	0.41	5.30	5.83
3	20.52%	0.46	4.34	4.93
4	18.39%	0.55	3.61	**4.29**
	O5EU ⋈ O6EU			
1	34.32%	5.83	30.55	38.01
2	27.97%	5.35	24.24	31.22
3	24.84%	6.06	21.55	29.24
4	22.60%	6.61	19.99	**28.23**
	O5NA ⋈ O6NA			
1	22.26%	3.56	24.08	28.49
2	17.58%	3.14	18.81	22.81
3	15.68%	3.65	17.13	21.64
4	14.45%	4.52	16.02	**21.40**
	O5SA ⋈ O6SA			
1	25.80%	0.17	1.44	1.66
2	20.74%	0.14	1.21	1.39
3	18.39%	0.17	1.12	1.33
4	17.03%	0.20	1.07	**1.30**
	O5OC ⋈ O6OC			
1	24.42%	0.10	1.51	1.65
2	18.89%	0.12	1.09	1.25
3	16.17%	0.14	0.95	1.13
4	14.65%	0.16	0.88	**1.08**

Table 10: # of partitions per dim. effect on APRIL size (MB).

#	T1	T2	T3	O5AF	O6AF	O5AS	O6AS	O5EU	O6EU	O5NA	O6NA	O5SA	O6SA	O5OC	O6OC
1	14.4	134.0	57.2	14.2	25.4	55.2	64.5	180.3	968.0	251.0	155.0	25.4	44.4	7.3	15.0
2	26.1	236.3	112.0	29.2	49.2	106.9	124.2	336.9	1900.0	453.4	311.8	51.5	86	14.3	49.2
3	37.1	352.6	166.7	44.7	74.2	164.0	188.3	492.5	2800.0	654.2	459.6	76.9	129.8	35.2	76.3
4	47.2	465.9	224.9	61.4	99.5	219.1	255.1	653.0	3700.0	875.1	619.0	104.2	172.3	49.1	107.7

Table 11: Join between T1 (order 16) and T3 (order N).

N	True hits	True negs.	Indecisive	Int. Filter (s)	Refinement (s)	Total (s)	T3 size (MB)
16	69.84%	28.13%	2.03%	0.19	0.33	0.57	57.2
15	69.63%	27.85%	2.52%	0.13	0.41	0.59	28.3
14	69.18%	27.46%	3.36%	0.11	0.54	0.70	14.0
13	68.39%	26.86%	4.75%	0.09	0.78	0.92	6.9
12	66.63%	25.70%	7.67%	0.09	1.23	1.37	3.4

one. The filter time also decreases, due to the reduced amount of intervals from T3 in the interval joins. However, the percentage of indecisive pairs increases, raising the refinement cost. $N = 15$ is the best value for T3, because it achieves the same performance as $N = 16$, while cutting the space requirements in half.

6.4 APRIL Construction Cost

We now evaluate the APRIL construction techniques that we have proposed in Section 5, comparing them with the rasterization method used in previous work [19, 56] that employs polygon clipping and polygon-cell intersection area computations. Table 12 shows the time taken to compute the APRIL approximations of all polygons in each dataset (for $N = 16$), using (i) the rasterization+intervalization approach of [19], after unifying Strong and Weak cells, (ii) the FloodFill approach tailored for APRIL presented in Section 5.1, and (iii) two versions of our novel OneStep intervalization approach

Table 12: Total construction cost (sec) for all datasets.

Dataset	[19]	FloodFill	OneStep (PiPs)	OneStep (Neighbors)
T1	143.62	3.90	3.74	**2.19**
T2	601.67	28.05	33.76	**23.43**
T3	9919.06	265.72	75.40	**28.33**
O5AF	264.45	**4.25**	11.00	4.72
O6AF	468.47	13.06	5.66	**4.17**
O5AS	486.86	**11.69**	21.28	11.78
O6AS	994.93	28.98	65.01	**25.07**
O5EU	1193.71	36.08	55.79	**33.71**
O6EU	5493.15	172.20	243.17	**156.94**
O5NA	1530.92	**53.33**	133.39	66.60
O6NA	1630.29	43.40	51.79	**30.71**
O5SA	361.87	**6.67**	14.74	6.77
O6SA	1478.05	34.56	22.86	**10.52**
O5OC	39.99	2.88	3.82	**2.49**
O6OC	113.99	9.32	20.75	**8.56**

(Section 5.2): one that performs a point-in-polygon (PiP) test for each first cell c of a candidate Full interval and one that checks the Neighbors of c before attempting the PiP test.

Observe that our OneStep intervalization algorithm employing the Neighbors check is the fastest approach in most of the cases. OneStep (Neighbors) applies 40% – 70% fewer PiP tests compared to OneStep (PiPs) that does not apply the Neighbors check. Only in a few datasets containing relatively small polygons OneStep (Neighbors) is up to 24% slower than the FloodFill method. On the other hand, in some datasets containing large polygons (e.g., T3, O6AF, O6SA) OneStep is up to one order of magnitude faster than FloodFill. Both methods proposed in Section 5 are orders of magnitude faster compared to previously applied rasterization techniques [19] mainly due to the simplicity of APRIL compared to previous raster-based intermediate filters [19, 56].

Comparison to IDEAL We also compared OneStep to the rasterization technique used in IDEAL [44], as implemented in [43]. We modified IDEAL's granularity definition formula accordingly to match APRIL's Hilbert space grid of order $N = 16$. For such high granularity, IDEAL demanded too much memory for most datasets and crashed, so we could only run it for three datasets as shown in Table 13. In all these cases, OneStep has 2x-3x lower cost compared to IDEAL's rasterization approach.

Table 13: Comparison with IDEAL's rasterization [44].

Dataset	One-Step (Neighbors)	IDEAL
T1	2.19	6.41
O5AF	4.72	10.80
O5OC	2.49	7.13

Applicability of OpenGL rasterization Finally, we have investigated the applicability of GPU-based rasterization approaches in the construction of APRIL approximations. For this, we tested an OpenGL implementation that uses a GPU (NVIDIA GeForce RTX 3060) and follows the approach described in [53] to identify Partial and Full cells of a polygon on a raster. OpenGL is an API that supports the graphics pipeline to perform efficient rasterization and drawing of the raster cells (pixels) into a frame buffer for visualization. In addition to rasterization, APRIL requires the retrieval of the cells' Hilbert curve identifiers and cell type information to create interval lists. Furthermore, OpenGL's rendering pipeline is designed to work with triangles, and thus we have to triangulate

all our input polygons before rendering. Finally, the resolution of the frame buffer plays a crucial role in rasterization accuracy.

The frame buffer 's resolution must match the desired granularity (i.e., $2^{16} \times 2^{16}$) of APRIL approximations. However, OpenGL does not allow frame buffers to have resolution higher than $2^{15} \times 2^{15}$ pixels, so APRIL approximations created using OpenGL are destined to have lower filter effectiveness than if they were created using our CPU-based methods (Section 5).

In addition, in our experiments, we have found that triangulation, which is a pre-requisite of using OpenGL's rendering, takes up 66% - 94% of the total rasterization time. For example, triangulating the T3 dataset in its entirety takes around 160 seconds, which is already about 6x more expensive than the end-to-end production of the APRIL approximations of all objects in T3 using our OneStep approach (see Table 12).

Overall, its limitations in setting an appropriate resolution and the high costs for initializing and postprocessing its rasterization process, make OpenGL-based APRIL construction suboptimal compared to our CPU-based algorithms.

7 RELATED WORK

Most previous works on spatial intersection joins [22] focus on the filter step of the join (denoted by MBR-join). They either exploit the pre-existing indexes [11, 27] or partition the data on-the-fly and perform the join independently at each partition [30, 35, 47]. Each partition-to-partition MBR-join can be performed in memory with the help of plane-sweep [5, 11].

Intermediate filters Finer (but more space-consuming) approximations have been proposed to be used in an intermediate filter step that identifies true negatives and/or true positives, as described in Section 2. The first work in this direction [10] proposed the use of simple convex polygons (convex hull and the minimum bounding 5-corner convex polygon (5C)). Another approach [38] extends the MBR to capture the empty space around its corners, which may help in the detection of false positives. Raster approximations of object MBRs have also been suggested, with a classification of the cells therein based on their coverage by the object [56]. Recently, this approach has been improved in [19] to (i) apply on a global grid, (ii) represent the cells as intervals with bitcodes of the cell types, (iii) perform the intermediate filter as a specialized interval join, as described in Section 2. A hierarchical raster approximation for window and distance queries was proposed in [18]. Raster approximations have also been combined with vector approximations in [44]. However, neither [18] nor [44] studied the spatial intersection join, for which the state-of-the-art intermediate filter is RI [19].

Refinement step Verifying whether two polygons overlap is CPU-intensive, requiring the application of an intersection detection algorithm between sets of line segments and two point-in-polygon tests [10]. To speed it up, Brinkhoff et al. [10] suggest decomposing polygons into sets of trapezoids while [6] suggests alternative polygon decomposition approaches. These techniques are orthogonal to APRIL, as they aim to speed up the refinement step, while APRIL reduces the number of candidate join pairs that require refinement.

Approximate spatial joins The approximate representation of objects and approximate spatial query evaluation using space-filling curves was first suggested by Orenstein [31]. Recent work explores the use of raster approximations for the approximate evaluation of spatial joins and other operations [23, 49, 54]. RI [19] and our work are the first to approximate polygon rasterizations as intervals for *exact* spatial query evaluation.

Spatial joins on GPUs The widespread availability of programmable GPUs has inspired several research efforts that leverage GPUs for spatial joins [1, 2, 25, 26, 42]. Sun et al. [42] accelerated the join refinement step by incorporating GPU rasterization as an intermediate filter. This filter identifies *only true negatives* using a low resolution, and has thus limited pruning effectiveness. Aghajarian et al. [1, 2] proposed a GPU approach to process point-polygon and polygon-polygon joins for datasets that can be accommodated in GPU memory. Liu et al. [25, 26] also proposed GPU-accelerated filters to reduce the number of refinements. These filters [1, 2, 25, 26], in contrast to APRIL, *do not identify true hits*, but rather focus on finding the intersection points between a candidate pair. Furthermore, the above approaches [1, 2, 25, 26] do not involve rasterization and rely on CUDA, which is exclusive to NVIDIA GPUs. A recent line of work [15, 16, 53, 54] proposes to use the GPU rasterization pipeline as an integral component of spatial query processing. Doraiswamy et al. [15, 16] introduced a spatial data model and algebra that is designed to exploit modern GPUs. Their approach leverages a data representation called *canvas*, which stores polygons as collections of pixels. The canvas includes a flag that differentiates between pixels that lie on the boundary of the polygon and those that are entirely covered by it. Although current-generation GPUs can handle millions of polygons at fast frame rates, the evaluation of spatial queries is still dominated by other costs, such as triangulating polygons and performing I/Os [16].

Scalability in spatial data management The emergence of cloud computing has led to many efforts to scale out spatial data management [33]. SJMP [55] is an adaptation of the PBSM spatial join algorithm [35] for MapReduce. Other spatial data management systems that use MapReduce or Spark and handle spatial joins include Hadoop-GIS [3], SpatialHadoop [17], Magellan [41], SpatialSpark [51], Simba [50], and Apache Sedona [52]. All the aforementioned systems focus only on the filter step of spatial joins.

8 CONCLUSIONS

We propose APRIL, an approximation technique for polygons, to use as an intermediate filter in the spatial intersection join pipeline. Compared to previous approaches [10, 19, 56], APRIL is (i) lightweight, as it represents each polygon by two lists of integers that can be effectively compressed; (ii) effective, as it typically filters the majority of MBR-join pairs as true negatives or true positives; and (iii) efficient to apply, as it only requires at most three linear scans over the interval lists. APRIL is a general approximation for polygons that can also be used in selection queries, within-joins and joins between polygons and linestrings. We propose a compression technique for APRIL and customizations that trade space for filter effectiveness. Finally, we propose efficient construction techniques for APRIL approximations, which greatly perform rasterization-based techniques from previous work. In the future, we plan to explore the integration of APRIL in a spatial database system, investigate further the problem of interval join order optimization for APRIL for candidate join pairs, and explore the effectiveness of APRIL for queries that involve 3D objects (e.g., polytopes).

REFERENCES

[1] Danial Aghajarian and Sushil K. Prasad. 2017. A Spatial Join Algorithm Based on a Non-uniform Grid Technique over GPGPU. In *Proceedings of the 25th ACM SIGSPATIAL International Conference on Advances in Geographic Information Systems, GIS 2017, Redondo Beach, CA, USA, November 7-10, 2017*, Erik G. Hoel, Shawn D. Newsam, Siva Ravada, Roberto Tamassia, and Goce Trajcevski (Eds.). ACM, 56:1–56:4.

[2] Danial Aghajarian, Satish Puri, and Sushil K. Prasad. 2016. GCMF: an efficient end-to-end spatial join system over large polygonal datasets on GPGPU platform. In *Proceedings of the 24th ACM SIGSPATIAL International Conference on Advances in Geographic Information Systems, GIS 2016, Burlingame, California, USA, October 31 - November 3, 2016*. ACM, 18:1–18:10.

[3] Ablimit Aji, Fusheng Wang, Hoang Vo, Rubao Lee, Qiaoling Liu, Xiaodong Zhang, and Joel H. Saltz. 2013. Hadoop-GIS: A High Performance Spatial Data Warehousing System over MapReduce. *Proc. VLDB Endow.* 6, 11 (2013), 1009–1020.

[4] John Amanatides and Andrew Woo. 1987. A Fast Voxel Traversal Algorithm for Ray Tracing. In *8th European Computer Graphics Conference and Exhibition, Eurographics 1987, Amsterdam, The Netherlands, August 24-28, 1987, Proceedings*. North-Holland / Eurographics Association.

[5] Lars Arge, Octavian Procopiuc, Sridhar Ramaswamy, Torsten Suel, and Jeffrey Scott Vitter. 1998. Scalable Sweeping-Based Spatial Join. In *VLDB'98, Proceedings of 24rd International Conference on Very Large Data Bases, August 24-27, 1998, New York City, New York, USA*, Ashish Gupta, Oded Shmueli, and Jennifer Widom (Eds.). Morgan Kaufmann, 570–581.

[6] Wael M. Badawy and Walid G. Aref. 1999. On Local Heuristics to Speed Up Polygon-Polygon Intersection Tests. In *ACM-GIS '99, Proceedings of the 7th International Symposium on Advances in Geographic Information Systems, November 2-6, 1999, Kansas City, USA*. ACM, 97–102.

[7] Boost. [n. d.]. Boost C++ Libraries. http://www.boost.org/.

[8] Jack Bresenham. 1965. Algorithm for Computer Control of a Digital Plotter. *IBM Syst. J.* 4, 1 (1965), 25–30.

[9] Thomas Brinkhoff, Hans-Peter Kriegel, and Ralf Schneider. 1993. Comparison of Approximations of Complex Objects Used for Approximation-based Query Processing in Spatial Database Systems. In *Proceedings of the Ninth International Conference on Data Engineering, April 19-23, 1993, Vienna, Austria*. IEEE Computer Society, 40–49.

[10] Thomas Brinkhoff, Hans-Peter Kriegel, Ralf Schneider, and Bernhard Seeger. 1994. Multi-Step Processing of Spatial Joins. In *Proceedings of the 1994 ACM SIGMOD International Conference on Management of Data, Minneapolis, Minnesota, USA, May 24-27, 1994*, Richard T. Snodgrass and Marianne Winslett (Eds.). ACM Press, 197–208.

[11] Thomas Brinkhoff, Hans-Peter Kriegel, and Bernhard Seeger. 1993. Efficient Processing of Spatial Joins Using R-Trees. In *Proceedings of the 1993 ACM SIGMOD International Conference on Management of Data, Washington, DC, USA, May 26-28, 1993*. ACM Press, 237–246.

[12] cruppstahl. 2017. *libvbyte - Fast C Library for 32bit and 64bit Integer Compression*. https://github.com/cruppstahl/libvbyte

[13] Douglas R. Cutting and Jan O. Pedersen. 1990. Optimizations for Dynamic Inverted Index Maintenance. In *SIGIR'90, 13th International Conference on Research and Development in Information Retrieval, Brussels, Belgium, 5-7 September 1990, Proceedings*. ACM, 405–411.

[14] Jens-Peter Dittrich and Bernhard Seeger. 2000. Data Redundancy and Duplicate Detection in Spatial Join Processing. In *Proceedings of the 16th International Conference on Data Engineering, San Diego, California, USA, February 28 - March 3, 2000*, David B. Lomet and Gerhard Weikum (Eds.). IEEE Computer Society, 535–546.

[15] Harish Doraiswamy and Juliana Freire. 2020. A GPU-friendly Geometric Data Model and Algebra for Spatial Queries. In *Proceedings of the 2020 International Conference on Management of Data, SIGMOD Conference 2020, online conference [Portland, OR, USA], June 14-19, 2020*. ACM, 1875–1885.

[16] Harish Doraiswamy and Juliana Freire. 2022. SPADE: GPU-Powered Spatial Database Engine for Commodity Hardware. In *38th IEEE International Conference on Data Engineering, ICDE 2022, Kuala Lumpur, Malaysia, May 9-12, 2022*. IEEE, 2669–2681.

[17] Ahmed Eldawy and Mohamed F. Mokbel. 2015. SpatialHadoop: A MapReduce framework for spatial data. In *31st IEEE International Conference on Data Engineering, ICDE 2015, Seoul, South Korea, April 13-17, 2015*, Johannes Gehrke, Wolfgang Lehner, Kyuseok Shim, Sang Kyun Cha, and Guy M. Lohman (Eds.). IEEE Computer Society, 1352–1363.

[18] Yi Fang, Marc T. Friedman, Giri Nair, Michael Rys, and Ana-Elisa Schmid. 2008. Spatial indexing in microsoft SQL server 2008. In *Proceedings of the ACM SIGMOD International Conference on Management of Data, SIGMOD 2008, Vancouver, BC, Canada, June 10-12, 2008*. 1207–1216.

[19] Thanasis Georgiadis and Nikos Mamoulis. 2023. Raster Intervals: An Approximation Technique for Polygon Intersection Joins. In *Proceedings of the 2023 ACM SIGMOD International Conference on Management of Data, Seattle, Washington, USA, June*.

[20] Antonin Guttman. 1984. R-Trees: A Dynamic Index Structure for Spatial Searching. In *SIGMOD'84, Proceedings of Annual Meeting, Boston, Massachusetts, USA, June 18-21, 1984*, Beatrice Yormark (Ed.). ACM Press, 47–57.

[21] David Hilbert. 1891. Über die stetige Abbildung einer Linie auf ein Flächenstück. *Mathematische Annalen* 38, 1 (1891), 459–460.

[22] Edwin H. Jacox and Hanan Samet. 2007. Spatial join techniques. *ACM Trans. Database Syst.* 32, 1 (2007), 7.

[23] Andreas Kipf, Harald Lang, Varun Pandey, Raul Alexandru Persa, Christoph Anneser, Eleni Tzirita Zacharatou, Harish Doraiswamy, Peter A. Boncz, Thomas Neumann, and Alfons Kemper. 2020. Adaptive Main-Memory Indexing for High-Performance Point-Polygon Joins. In *Proceedings of the 23rd International Conference on Extending Database Technology, EDBT 2020, Copenhagen, Denmark, March 30 - April 02, 2020*. OpenProceedings.org, 347–358.

[24] Daniel Lemire and Leonid Boytsov. 2012. Decoding billions of integers per second through vectorization. *CoRR* abs/1209.2137 (2012).

[25] Yiming Liu and Satish Puri. 2020. Efficient Filters for Geometric Intersection Computations using GPU. In *SIGSPATIAL '20: 28th International Conference on Advances in Geographic Information Systems, Seattle, WA, USA, November 3-6, 2020*, Chang-Tien Lu, Fusheng Wang, Goce Trajcevski, Yan Huang, Shawn D. Newsam, and Li Xiong (Eds.). ACM, 487–496.

[26] Yiming Liu, Jie Yang, and Satish Puri. 2019. Hierarchical Filter and Refinement System Over Large Polygonal Datasets on CPU-GPU. In *26th IEEE International Conference on High Performance Computing, Data, and Analytics, HiPC 2019, Hyderabad, India, December 17-20, 2019*. IEEE, 141–151.

[27] Nikos Mamoulis and Dimitris Papadias. 2003. Slot Index Spatial Join. *IEEE Trans. Knowl. Data Eng.* 15, 1 (2003), 211–231.

[28] Ken Museth. 2014. Hierarchical digital differential analyzer for efficient raymarching in OpenVDB. In *Special Interest Group on Computer Graphics and Interactive Techniques Conference, SIGGRAPH '14, Vancouver, Canada, August 10-14, 2014, Talks Proceedings*. ACM, 40:1.

[29] Sadegh Nobari, Qiang Qu, and Christian S. Jensen. 2017. In-Memory Spatial Join: The Data Matters!. In *Proceedings of the 20th International Conference on Extending Database Technology, EDBT 2017, Venice, Italy, March 21-24, 2017*. OpenProceedings.org, 462–465.

[30] Sadegh Nobari, Farhan Tauheed, Thomas Heinis, Panagiotis Karras, Stéphane Bressan, and Anastasia Ailamaki. 2013. TOUCH: in-memory spatial join by hierarchical data-oriented partitioning. In *Proceedings of the ACM SIGMOD International Conference on Management of Data, SIGMOD 2013, New York, NY, USA, June 22-27, 2013*. ACM, 701–712.

[31] Jack A. Orenstein. 1989. Redundancy in Spatial Databases. In *Proceedings of the 1989 ACM SIGMOD International Conference on Management of Data, Portland, Oregon, USA, May 31 - June 2, 1989*. ACM Press, 295–305.

[32] Varun Pandey, Andreas Kipf, Thomas Neumann, and Alfons Kemper. 2018. How Good Are Modern Spatial Analytics Systems? *Proc. VLDB Endow.* 11, 11 (2018), 1661–1673.

[33] Varun Pandey, Andreas Kipf, Thomas Neumann, and Alfons Kemper. 2018. How Good Are Modern Spatial Analytics Systems? *Proc. VLDB Endow.* 11, 11 (2018), 1661–1673.

[34] George Papadakis, Georgios M. Mandilaras, Nikos Mamoulis, and Manolis Koubarakis. 2021. Progressive, Holistic Geospatial Interlinking. In *WWW '21: The Web Conference 2021, Virtual Event / Ljubljana, Slovenia, April 19-23, 2021*. ACM / IW3C2, 833–844.

[35] Jignesh M. Patel and David J. DeWitt. 1996. Partition Based Spatial-Merge Join. In *Proceedings of the 1996 ACM SIGMOD International Conference on Management of Data, Montreal, Quebec, Canada, June 4-6, 1996*. ACM Press, 259–270.

[36] Suprio Ray, Bogdan Simion, Angela Demke Brown, and Ryan Johnson. 2014. Skew-resistant parallel in-memory spatial join. In *Conference on Scientific and Statistical Database Management, SSDBM '14, Aalborg, Denmark, June 30 - July 02, 2014*. ACM, 6:1–6:12.

[37] Mikio Shinya and Marie-Claire Forgue. 1991. Interference detection through rasterization. *Comput. Animat. Virtual Worlds* 2, 4 (1991), 132–134.

[38] Darius Sidlauskas, Sean Chester, Eleni Tzirita Zacharatou, and Anastasia Ailamaki. 2018. Improving Spatial Data Processing by Clipping Minimum Bounding Boxes. IEEE Computer Society, 425–436.

[39] Alvy Ray Smith. 1979. Tint fill. In *Proceedings of the 6th Annual Conference on Computer Graphics and Interactive Techniques, SIGGRAPH 1979, Chicago, Illinois, USA, August 8-10, 1979*, Thomas A. DeFanti, Bruce H. McCormick, Bary W. Pollack, Norman I. Badler, and S. H. Chasen (Eds.). ACM, 276–283.

[40] SpatialHadoop. 2015. *TIGER datasets*. http://spatialhadoop.cs.umn.edu/datasets.html

[41] Ram Sriharsha. [n. d.]. Magellan: Geospatial Analytics Using Spark. https://github.com/harsha2010/magellan.

[42] Chengyu Sun, Divyakant Agrawal, and Amr El Abbadi. 2003. Hardware Acceleration for Spatial Selections and Joins. In *Proceedings of the ACM SIGMOD International Conference on Management of Data, San Diego, California, USA*. ACM, 455–466.

[43] Dejun Teng. 2021. *IDEAL*. https://github.com/tengdj/IDEAL

[44] Dejun Teng, Furqan Baig, Qiheng Sun, Jun Kong, and Fusheng Wang. 2021. IDEAL: a Vector-Raster Hybrid Model for Efficient Spatial Queries over Complex Polygons. In *22nd IEEE International Conference on Mobile Data Management, MDM 2021, Toronto, ON, Canada, June 15-18, 2021*. IEEE, 99–108.

[45] Konstantinos Theocharidis, John Liagouris, Nikos Mamoulis, Panagiotis Bouros, and Manolis Terrovitis. 2019. SRX: efficient management of spatial RDF data. *VLDB J.* 28, 5 (2019), 703–733.

[46] Larry H. Thiel and H. S. Heaps. 1972. Program design for retrospective searches on large data bases. *Inf. Storage Retr.* 8, 1 (1972), 1–20.

[47] Dimitrios Tsitsigkos, Panagiotis Bouros, Nikos Mamoulis, and Manolis Terrovitis. 2019. Parallel In-Memory Evaluation of Spatial Joins. In *Proceedings of the 27th ACM SIGSPATIAL International Conference on Advances in Geographic Information Systems, SIGSPATIAL 2019, Chicago, IL, USA, November 5-8, 2019*. ACM, 516–519.

[48] Dimitrios Tsitsigkos, Konstantinos Lampropoulos, Panagiotis Bouros, Nikos Mamoulis, and Manolis Terrovitis. 2021. A Two-layer Partitioning for Non-point Spatial Data. In *37th IEEE International Conference on Data Engineering, ICDE 2021, Chania, Greece, April 19-22, 2021*. IEEE, 1787–1798.

[49] Christian Winter, Andreas Kipf, Christoph Anneser, Eleni Tzirita Zacharatou, Thomas Neumann, and Alfons Kemper. 2021. GeoBlocks: A Query-Cache Accelerated Data Structure for Spatial Aggregation over Polygons. In *Proceedings of the 24th International Conference on Extending Database Technology, EDBT 2021, Nicosia, Cyprus, March 23 - 26, 2021*. OpenProceedings.org, 169–180.

[50] Dong Xie, Feifei Li, Bin Yao, Gefei Li, Liang Zhou, and Minyi Guo. 2016. Simba: Efficient In-Memory Spatial Analytics. In *Proceedings of the 2016 International Conference on Management of Data, SIGMOD Conference 2016, San Francisco, CA, USA, June 26 - July 01, 2016*, Fatma Özcan, Georgia Koutrika, and Sam Madden (Eds.). ACM, 1071–1085.

[51] Simin You, Jianting Zhang, and Le Gruenwald. 2015. Large-scale spatial join query processing in Cloud. In *CloudDB, ICDE Workshops*. 34–41.

[52] Jia Yu, Zongsi Zhang, and Mohamed Sarwat. 2019. Spatial data management in apache spark: the GeoSpark perspective and beyond. *GeoInformatica* 23, 1 (2019), 37–78.

[53] Eleni Tzirita Zacharatou, Harish Doraiswamy, Anastasia Ailamaki, Cláudio T. Silva, and Juliana Freire. 2017. GPU Rasterization for Real-Time Spatial Aggregation over Arbitrary Polygons. *Proc. VLDB Endow.* 11, 3 (2017), 352–365.

[54] Eleni Tzirita Zacharatou, Andreas Kipf, Ibrahim Sabek, Varun Pandey, Harish Doraiswamy, and Volker Markl. 2021. The Case for Distance-Bounded Spatial Approximations. In *11th Conference on Innovative Data Systems Research, CIDR 2021, Virtual Event, January 11-15, 2021, Online Proceedings*. www.cidrdb.org.

[55] Shubin Zhang, Jizhong Han, Zhiyong Liu, Kai Wang, and Zhiyong Xu. 2009. SJMR: Parallelizing spatial join with MapReduce on clusters. In *Proceedings of the 2009 IEEE International Conference on Cluster Computing, August 31 - September 4, 2009, New Orleans, Louisiana, USA*. IEEE Computer Society, 1–8.

[56] Geraldo Zimbrao and Jano Moreira de Souza. 1998. A Raster Approximation For Processing of Spatial Joins. In *VLDB'98, Proceedings of 24rd International Conference on Very Large Data Bases, August 24-27, 1998, New York City, New York, USA*. 558–569.